GENERATING MULTIPLE SUPERRADIANCE PULSES IN A SLIPPAGE-DOMINANT FREE-ELECTRON LASER AMPLIFIER

X. Yang, Y. Shen,
National Synchrotron Light Source, Brookhaven National Laboratory, Upton, NY 11973, USA

Abstract

We report the first numerical demonstration of the generation of multiple superradiance pulses in a slippage-dominant free-electron laser amplifier. In this simulation, the 1st and 2nd multiple radiation-pulses are created from the deformation of the longitudinal phase space. Our simulation confirmed controllability over the temporal profile of these pulses, and paves the way for applying this technique, such as generating multiple pulses for slippage-dominant laser-seeded FELs.

INTRODUCTION

The free-electron laser (FEL) is a tunable source of coherent radiation, ranging from terahertz (THz) waves to hard X-rays, with the capability for femtosecond time-resolution. Progress was made recently in single-pass FELs in moving toward the X-ray region of the spectrum, such as the self-amplified spontaneous emission (SASE) FEL that successfully lased from soft X-rays down to 1.5Å [1,2], the laser-seeded FEL amplifier [3], and the high-gain harmonic generation (HGHG) FEL [4] that emitted radiation in the deep ultraviolet (DUV), i.e., below 300nm. One of the main advantages of the HGHG and laser-seeded FEL over the SASE FEL is that they produce temporally as well as transversely coherent pulses. In contrast, SASE radiation starts from the initial shot-noise of the electron beam, so that the resulting radiation exhibits excellent spatial but a rather poor temporal coherence.

In this report, we present numerical evidence for a new slippage-dominant superradiance FEL interaction regime, wherein the emitted FEL pulse is followed by multiple pulses, which we dubbed a "multi-pulse regime". This dynamic behavior occurs in seeded FELs where the duration of the seed pulse is short; it may be important for next-generation short-wavelength-seeded FELs, such as FERMI [5], and LCLS-II [6]. Understanding control of these regimes is essential for optimizing the power and quality of the FEL sources, features demanded by the user communities. Using the Perseo simulation [7], we investigated the behavior of the seeded FEL, and obtained new insights on multiple-pulse generation that we interpreted in terms of the deformation of the longitudinal phase space (LPS) and the formation of new buckets. Here, the term "bucket" denotes the electric field of an optical pulse that assures longitudinal focusing, thereby constraining the electron's motion to a stable region in the LPS.

The mechanism of FEL amplification commonly is analyzed in three steps [8]: (i) energy modulation [9], (ii) exponential growth, and (iii) saturation. In the first evolutionary step, energy is exchanged between the electrons and the radiation, leading to an energy modulation, and further, to a density modulation (microbunching) of the electrons at the resonant wavelength $\lambda_r = \lambda_w(1+K^2/2) / (2\gamma_r^2)$, determined by the electron beam's energy $E_r=mc^2\gamma_r$. $K = eB_w/mck_w$ is the dimensionless undulator parameter, and λ_w, k_w, and B_w are, respectively, the undulator's wavelength, wave number, and magnetic field [11]. Using a coherent seed to initiate the FEL process enables us to lock in the phase of the microbunches and to achieve much better temporal coherence. Afterwards, the FEL enters the second evolutionary step in which the radiated power increases exponentially to the detriment of the electron beam's kinetic energy. The strong energy losses, corresponding to a redshift of λ_r, thereafter disable interaction between the electron and the radiation field. In steady state, the FEL reaches a maximum power and saturates. Its final characteristics (power, duration, spectral width) depend only on the parameters of the undulator and electron beam. Taking time-dependence into account, the optical pulse slips forward with respect to the electron beam by one wavelength λ per undulator period, resulting in the so-called slippage regime characterized by the slippage length $\delta_s = N_w\lambda$. δ_s is the displacement of the optical pulse with respect to the electron beam at the end of the N_w periods of the undulator. The slippage-dominant superradiance regime [12] is characterized by the propagation of a solitary wavelike pulse where the power of the optical pulse (main pulse) grows quadratically with time and its pulse length decreases [13,14,15], resulting in a decrease in the interaction length where the electrons overlap with the main pulse and thereby limiting the output power. However, the interaction length can be extended *via* generating multiple pulses. Here, the multi-pulse regime covers the entire slippage distance along the electron bunch except the part overlapping the seed- and main- radiation pulses [Fig. 1]. Numerical studies reveal that LPS fragmentation and the formation of new buckets are core ingredients of the multi-pulse dynamics. In these circumstances, an ultra-short seed-pulse induces microbunching only when it slips over the electrons at $v_g \sim c$ [12]. Microbunching induces coherent emission from the electrons, forming the main radiation pulse and leaving behind those electrons with a large energy spread. Afterwards, they shear in phase due to intrinsic dispersion [9,10]. The low-energy part ($p < 0$) having more electrons [≥70%, obtained by counting the number of particles in the low-energy part *vs*. the total number of particles distributed within (-π, π)] and, accordingly, a larger bunching coefficient than the high-energy part, emits

ISBN 978-3-95450-123-6

coherent light to become a new pulse. Here, $p = (E-E_0) / \rho \cdot E_0$ is the energy variation with respect to the reference particle E_0, and ρ is the FEL Pierce parameter [9,10] characterizing the gain of the FEL. The above process is repeated [a fraction (≤50%, similarly obtained by counting the particles) of the bunched electrons left behind by the new pulse still can emit coherent light], generating additional pulses. We demonstrate that this configuration enables us to extend the FEL's interaction to a wider range in the slippage region, and eventually creates complex temporal-structural formation, such as multiple radiation pulses.

In this paper, we numerically explore the generation and suppression of multiple superradiance pulses in a single-pass FEL amplifier. We analyze FEL evolution from the viewpoint of electron longitudinal phase-space, showing the relation between the synchrotron oscillation and the structure of the radiation pulse. We detail how this mechanism could be applied to increase the radiation output or to suppress multiple pulses after the main pulse, so obtaining a clean output pulse. We support our analysis via simulations obtained with the well-known and established simulation code Perseo, employing it to resolve the one-dimensional (1D) FEL model, including the high-order harmonics described by the one-dimensional Colson -Bonifacio model [9,16] :

$$\frac{\partial \phi_j}{\partial \bar{z}} = p_j, \tag{1a}$$

$$\frac{\partial p_j}{\partial \bar{z}} = -\left[A(\bar{z},\tau) e^{i\phi_j} + c.c. \right], \tag{1b}$$

$$\left(\frac{\partial}{\partial \bar{z}} + \frac{\partial}{\partial \tau} \right) A(\bar{z},\tau) = \chi(\tau) b(\bar{z},\tau). \tag{1c}$$

Each particle j, j=1…N_e wherein N_e, the total number of electrons in the optical field A, is followed in the phase space using φ_j, the particle's relative phase, and p_j, the particle's relative energy, both normalized to the reference particle. The variables φ_j, p_j, and A are functions of the longitudinal coordinates τ along the electron bunch, and $\bar{z}$ along the undulator. τ is defined within $0 < \tau < L_e$, with L_e the electron bunch's length, and $\bar{z}$ is defined within $0 < \bar{z} < L_w$, with L_w the undulator length. All dimensions are in cooperation length [13,16] units: $l_c = \lambda/4\pi\rho$. χ is the macroscopic electronic-density normalized to 1, and $b(\bar{z}, \tau)$ is the bunching coefficient: $b(\bar{z}, \tau) = (1/N) \Sigma e^{-i\varphi j}$. Equations (1a) and (1b) describe the particle's dynamics, while Eq. (1c) includes the pulse's propagation.

SIMULATION

The initial condition for the slippage-dominant superradiance regime is defined more precisely in scaled units using S_{seed} ($=4\pi\rho N_w/L_{seed}$), the ratio of the slippage length to duration of the seed pulse, S_e ($=4\pi\rho N_w/L_e$), the ratio of the slippage length to the electron-bunch's length [17], and F_{seed} ($=\Delta f_{FWHM}/f_0 \cdot \rho$), the ratio of the seed's spectral bandwidth and the FEL-gain's bandwidth. Within the short seed pulse limit, S_e<<1 is chosen to have a nearly constant electron current in the simulation window, while S_{seed}>>1 and F_{seed}>>1 satisfy the slippage-dominant superradiance condition, where the bandwidth of the seed laser is much larger than that of the FEL gain. Therefore, when the seed pulse slips over the electron bunch at $v_g \sim c$, it only microbunches the electrons [12].

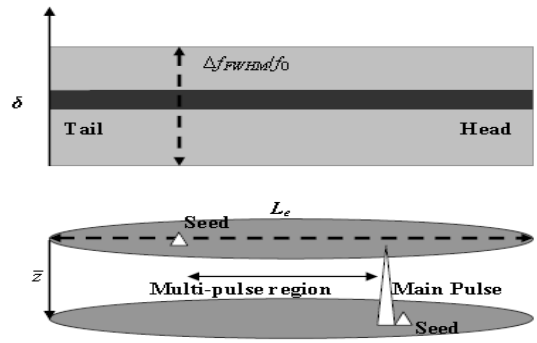

Figure 1: Schematic of the seeded-FEL's initial parameters. $\bar{z}$ is the longitudinal coordinate along the undulator. L_e and $\delta = (E-E_r) / \rho \cdot E_r$ are, respectively, the electron bunch's length and energy detuning. Here, $E_r = E_0$. Δf_{FWHM} is bandwidth of the seed laser.

Eq. (1) is used to simulate the evolution of the FEL in the regime of a long electron bunch and slippage-dominant superradiance, i.e., S_e<<1, S_{seed}>>1, and F_{seed}>>1. Figure 2 illustrates the dynamics of the FEL pulse via 2D diagrams where the longitudinal coordinate along the electron bunch, τ, is plotted on the horizontal axis and the coordinate along the undulator $\bar{z}$ on the vertical axis.

Figure 2(a) depicts the evolution of the FEL into the superradiance regime [14,18,19]. The seed pulse provides microbunching to the electrons only when it slips over them at $v_g \sim c$, and maintains its pulse shape and amplitude in the undulator. Microbunching emits coherent light that grows exponentially in intensity. At the end of exponential growth and the beginning of superradiance ($\bar{z} \approx 2.6$ in the undulator), the main pulse slips, as in the exponential regime, ahead of the electron bunch at $v_g \sim c$ instead of at $v_g \sim c/3$, while the length of the pulse decreases and the amplitude increases quadratically with the distance along the undulator. Simultaneously, it induces strong microbunching of the electrons. At a given delay in time, the 1st multiple pulse appears weaker in amplitude compared to the main pulse, similar to the case for the 2nd multiple pulse.

To investigate the origin of multiple pulses, we studied the evolution of the particle's relative longitudinal position (phase). Indeed, the constructive phase relationship indicates the formation of a new pulse. For FELs, the gain medium consists of relativistic electrons and the extent to which the phase of the microbunches is locked and sheared along the undulator determines the optical field's temporal profile. The phase shift is caused by energy modulation and the FEL's intrinsic dispersion.

ISBN 978-3-95450-123-6

The original reference particle, corresponding to the original bucket center, and also being the reference for the simulation, is fixed in LPS due to the zero energy offset [δ_0 (= (E_0-E_r) / $\rho \cdot E_r$)=0]. Here, the bucket center refers to the stable fixed point in the LPS [20]. However, this not the case for the new reference particle, corresponding to the new bucket center. Rather, it is fixed inside the new bucket but not in the LPS because it has a negative energy-offset (δ<0) with respect to the original reference particle. It shears toward the direction of the main pulse's tail. Whenever it shears the phase $\Delta\varphi$ across an integer of 2π, a new multiple pulse appears. $\Delta\varphi_n \approx n \cdot 2\pi$, n = 1, 2, .., corresponds, respectively, to the 1st, 2nd, .., multiple pulse. As confirmation, Fig. 2(b) show the LPS of the electrons at the newly formed buckets corresponding to the 1st and 2nd multiple pulses at the undulator distance, $\bar{z}$ = 12.8. Their phase changes relative to reference particle are ~2π and 4π, as indicated by the black dashed lines in Fig. 2(b), confirming that the constructive phase relationship is coincident with the formation of a new pulse. The time separation, Δt_n, between the nth multiple pulse and the main pulse is estimated using Eq. (2), derived straightforwardly from Eq. (1a).

$$\Delta t_n = {n \cdot \lambda_r} \Big/ {2 \cdot \delta_n \cdot c} \qquad (2)$$

As an example [Fig. 2(c)], the FEL Pierce parameter ρ = 0.004 and λ_r = 800nm, for n = 1, $\delta_1 \approx 5.0$ [Fig. 2(b)], the Δt_1 calculated using Eq. (2) is ~67fs, which is consistent with the result ~60fs obtained from the simulation [Fig. 2(c)].

An understanding of the physical mechanism behind the multi-pulse regime is gained by analyzing the electron's LPS at different positions along the radiation pulse. At the undulator position $\bar{z}$ = 12.8, we obtain the LPS of the electron beam (top), and of the overlapping optical pulse (bottom), as shown in Fig. 2(c). At position A, we show the LPS of electrons that the seed pulse has reached and that have only energy modulation. At position B, the effect of the interaction with the optical pulse is evident, such that a strong modulation in energy and density has occurred. On average, the electrons lose energy that is absorbed by the main pulse. At position C, corresponding to the peak of the main pulse, the electrons have reached the bottom of the bucket in phase space, and begin to gain energy from the laser field of the main pulse. Therefore, the power of the laser starts to drop and reaches a minimum at position D, where the corresponding phase space appears deeply saturated and the electrons start to become detrapped by the reduced ponderomotive potential. The strong optical field of the main pulse maximizes microbunching, and also causes a ~5% (ρ = 0.004) spread in the beam's energy, both of which are important to the generation of multiple pulses. At position E, the electrons are detrapped from the bottom energy after the passage of the main pulse, and are free to start a new process of FEL amplification. Those electrons close to the energy bottom form a new bucket in the series (black dashed circle) that is responsible for generating a new pulse. In addition to the shear in phase brought about by the energy spread and intrinsic dispersion, the majority of the electrons in new buckets arriving at the energy bottom after losing energy to the new pulse generate the peak of the new pulse [see position F]. Similar to the main pulse, the electrons already at the bottom of the bucket start to gain energy from the optical field of the new pulse. The energy of the new pulse starts to fall, and reaches a minimum at position G.

Overmodulation is the signature of local saturation: the bunch slices initially under the peak of the main pulse, modulated by the highest optical field, reach saturation in the undulator, and afterwards are detrapped due to the decline in intensity at the main pulse's tail edges. Electrons, detrapped from original bucket, shearing in z, and retrapped to new bucket, are responsible for generating the new pulse. Since the electrons carry on their rotation in LPS within the optical pulse's electric field, the process is repeated and additional pulses are generated. The radiation power of the multiple pulses continuously degrades to weaker levels, $P_n \approx a \cdot P_{n-1}$ ($a \leq$ 0.25) since a significant amount of the available electron kinetic energy has already been transferred to the earlier pulses. In addition, only a fraction (≤ 50%) of the low energy portion of the electrons participates in generating the new pulse, as shown in Figs. 2(a) - (c). The output power is proportional to the square of the beam's current ($P \sim I^2$) in the superradiance regime. Here, P_n is the FEL power integrated over the n^{th} pulse, and I is the electron-beam's current that contributes to the FEL output.

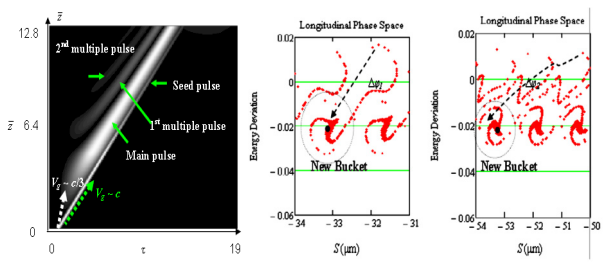

Figure 2(a): (left) Normalized longitudinal profile of the radiation power along the electron's coordinate, τ, as it evolves along the undulator with coordinate $\bar{z}$. Seed parameters: S_{seed} = 21 (with Gaussian shape, σ_{seed} = 0.26), and F_{seed} = 25 ($\Delta f_{FWHM}/f_0$=0.1, ρ = 0.004). Maximum seed field amplitude at $\bar{z}$ = 0: A_0 = 20. Initially: θ_j uniformly distributed within [-π, π] and p_j following a normal distribution center around zero with standard deviation 0.01%-RMS. σ_e = 88, corresponding to S_e = 0.06. Figure 2(b): (right) At $\bar{z}$ = 12.8 in the undulator, the LPS of the electrons at the positions where the peaks of the 1st (left) and 2nd (right) multiple pulses are. $\Delta\varphi_1 \approx 2\pi$, and $\Delta\varphi_2 \approx 4\pi$. In Figs. 2(b) and 2(c), energy deviation is calculated using the formula (E-E_0)/E_0, and the horizontal axis is the longitudinal position S in unit of μm.

ISBN 978-3-95450-123-6

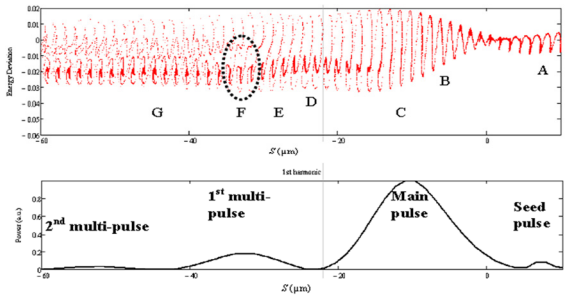

Figure 2(c): At $\bar{z}$ = 12.8 in the undulator, the LPS of the electron bunch (top), and the temporal profile of the radiation field along the electron coordinate (bottom). Separation between the main and 1st pulses is ~60fs, and between 1st and 2nd pulses it is ~70fs. The oval area enclosed by the black dashes signifies the bucket series that are responsible for generating the 1st multiple pulse.

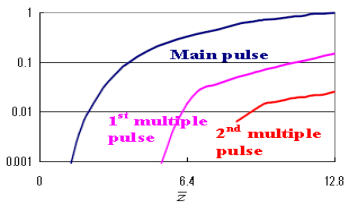

Figure 3: (color online) Evolution of the intensity of the FEL pulse along the undulator calculated using Eq. (1). Intensity integrated over the main pulse (blue), 1st multiple pulse (magenta), and 2nd multiple pulse (red).

Figure 3 illustrates the evolution of the FEL power (integrated over radiation pulse) along the undulator for three individual pulses, the main pulse (blue), the 1st multiple pulse (magenta), and the 2nd multiple pulse (red). It confirms that for each radiation pulse, the FEL power first increases exponentially and does not saturate. Rather, its amplification evolves as $\bar{z}^2$ [14,15,18,19]. The slippage enables us to propel the main pulse forward into the "fresh" electron region that maintains the feeding of the pulse. However, a similar slippage only pushes a multiple pulse forward into the region where the electrons already have lost energy to the radiation pulses ahead of it. Therefore, the output power of a multiple pulse is weaker than that of the pulse ahead of it. The undulator's length can be used as a control parameter to choose between increasing the radiation output [larger $\bar{z}$ (>5.12) is better] or suppressing the multiple pulses after the main pulse ($\bar{z} \leq 5.12$).

CONCLUSION

In conclusion, depending on the initial conditions (the parameters of the electron beam, undulator, and seed laser), the short-pulse-seeded FEL can be driven into different temporal and intensity regimes. We addressed a new regime in deeply saturated slippage-dominant FELs, wherein the multiple superradiance pulses following the main pulse can be either enhanced or suppressed. Multiple-pulse generation results from deformation of the LPS and the formation of new buckets. Furthermore, we demonstrated, both numerically and analytically, that the formation of a new pulse is closely related to the constructive phase-change ($\Delta\varphi_n \approx n \cdot 2\pi$, n = 1, 2, ..) between the original bucket center and the newly developed one. Therefore, the separation Δt between two adjacent pulses can be controlled via the Pierce parameter and (or) the parameters of the seed laser, since they both can alter the energy spread of the electron beam. While multiple pulses enhance FEL power, such a phenomenon might spoil the temporal profile of the radiation. Even though we can avoid multiple pulses by modulating the parameters of the electron beam and undulator, this choice is a tradeoff between the cleanness of the temporal profile and the FEL output power.

We gratefully acknowledge useful discussions with L. Giannessi, S. Hulbert, B. Podobedov, and A. Woodhead. We are thankful for support from the NSLS. This work is supported in part by U. S. Department of Energy (DOE) under contract No. DE-AC02-98CH1-886.

REFERENCES

[1] P. Emma (LCLS team), Nature Photonics **4**, 641 (2010).
[2] W. Ackermann *et al.*, Nat. Photon. **1**, 336 (2007).
[3] G. Lambert *et al.*, Nature Phys. **4**, 296 (2008).
[4] L. H. Yu *et al.*, Science 289, 932-934 (2000).
[5] E. Allaria *et al.*, *Proceedings of FEL 2006*, (BESSY, Berlin, Germany, 2006), p. 166.
[6] P. Emma (LCLS team), Nat. Photon. **4**, 641 (2010).
[7] L. Giannessi, *Proceedings of FEL 2006*, (BESSY, Berlin, Germany, 2006), p. 91.
[8] L. H. Yu, Phys. Rev. A **44**, 5178 (1991).
[9] R. Bonifacio *et al.*, Opt. Commun. **50**, 373 (1984).
[10] R. Bonifacio *et al.*, Phys. Rev. Lett. **73**, 70 (1994).
[11] W. B. Colson, IEEE J. Quantum Electron. **17**, 1417 (1981).
[12] X. Yang *et al.*, Phys. Rev. E **85**, 026404 (2012).
[13] R. Bonifacio *et al.*, Phys. Rev. A **44**, 3441 (1991).
[14] R. Bonifacio *et al.*, Nucl. Instrum. Methods Phys. Res. A **296**, 358 (1990).
[15] L. Giannessi *et al.*, J. Appl. Phys. **98**, 043110 (2005).
[16] W. B. Colson, Phys. Lett. A **59**, 187 (1976).
[17] M. Labat *et al.*, Phys. Rev. Lett. **103**, 264801 (2009).
[18] D. A. Jaroszynski *et al.*, Phys. Rev. Lett. **78**, 1699 (1997).
[19] T. Watanabe *et al.*, Phys. Rev. Lett. **98**, 034802(2007).
[20] S. Y. Lee, *Accelerator Physics*, World Scientific Publishing Co. Pte. Ltd. (1999).

ISBN 978-3-95450-123-6